# Numerical techniques for efficient sonar bearing and range searching in the near field using genetic algorithms

D.J. Edwards and A.J. Keane

November 19, 1996

Department of Engineering Science,
University of Oxford,
Parks Road, Oxford, OX1 3PJ, U.K.
and
Department of Mechanical Engineering,
University of Southampton,
Highfield, Southampton, SO17 1BJ, U.K.

**Abstract**

This article describes a numerical method that may be used to efficiently locate and track underwater sonar targets in the near-field, with both bearing and range estimation, for the case of very large passive arrays. The approach used has no requirement for *a priori* knowledge about the source and uses only limited information about the receiver array shape. The role of sensor position uncertainty and the consequence of targets always being in the near-field are analysed and the problems associated with the manipulation of large matrices inherent in conventional eigenvalue type algorithms noted. A simpler numerical approach is then presented which reduces the problem to that of search optimization. When using this method the location of a target corresponds to finding the position of the maximum weighted sum of the output from all sensors. Since this search procedure can be dealt with using modern stochastic optimization methods, such as the genetic algorithm, the operational requirement that an acceptable accuracy be achieved in real time can usually be met.

The array studied here consists of 225 elements positioned along a flexible cable towed behind a ship with 3.4m between sensors, giving an effective aperture of 761.6m. For such a long array, the far field assumption used in most beam-forming algorithms is no longer appropriate. The waves emitted by the targets then have to be considered as curved rather than plane. It is shown that, for simulated data, if no significant noise occurs in the same frequency band as the target signal, then bearing and range can be estimated with negligible error. When background noise is present (at -14dB), the target can normally still be located to within 1% in bearing and to around 5% error in range. Array shape uncertainty worsens this performance but it is shown that it is still possible to accurately determine the target bearing and to provide approximate estimates of range in such circumstances. Finally, the ability of the approach to track the sources over a period of time and with evolving array shape is demonstrated.

This work was supported by the Defence Research Agency under contract DRA-CB/CEN/9/4/2057/155/A

# 1 INTRODUCTION

In most published beam-forming and target location algorithms, there is an assumption that the sources are far from the array so that a planar wave-front approximation is possible. Moreover, it is also normal to assume that the array transducer positions are known with complete accuracy. In these circumstances eigen-decomposition high resolution methods [11] have proven to be effective means of obtaining bearing estimates of far-field narrow-band sources from noisy measurements. The performance of these algorithms is, in general, severely degraded when the target is in the near-field or there is uncertainty in the transducer positions. There is therefore a need to look again at the particular problems which arise in the case of flexible arrays of the order of a kilometre in length where the targets are effectively still in the near-field of the array for distances greater than 100 km and where sensor positions are never known precisely.

Techniques for estimating the directions-of-arrival (DOA) of signals impinging on antenna arrays have been investigated intensively over the years [10]. Beam-forming [24] is the most widely used processing technique for these arrays and can be used for direction finding by 'steering the beam' until the array output power is maximized (or minimized). The direction at which the power is maximized provides an estimate of the source bearing. In this approach, antenna arrays need to be calibrated to produce reliable DOA estimates. During the calibration process, the array response vector (also called the array manifold) is measured and stored, for a finite number of directions [18]. This response description depends on the amplitude and phase weighting of the signals from each element or sensor of the array and the positions of the elements within the array structure. It has been suggested that the array manifold be stored in the form of a set of vectors, for a grid of DOAs and frequencies spanning the desired field of view and the frequency band of interest [9]. However, very little work seems to have been done for the near-field case. Here, for point sources, the wave-front presented to the array is spherical and offers the additional degree of freedom of range variation. Also, any sensor position uncertainty presents an effective noise source and an investigation into its role in the beam-forming process needs to be undertaken to identify both the nature and magnitude of its effect. It is therefore desirable that a technique be developed that locates targets without prior knowledge of the array manifold or the number of sources, in a way that minimizes the computational effort and number of parameters to be estimated. It is also required that the technique be robust enough to perform satisfactorily when the signals are corrupted by background noise or uncertainty in sensor positions.

# 2 SIGNAL CONDITIONING - FILTERING AND AVERAGING

When performing sonar target identification and location, in the absence of noise, it is possible to determine the target position from a single set of sensor responses at any instant in time, given that the sensor locations are known. When there is noise present, due to background ocean noise, hydrodynamic flow noise, etc., or perhaps because the sensor locations fluctuate in an ill-determined manner with time, some form of averaging or matched filtering is required to improve the effectiveness of the process. Such averaging can occur over the set of sensors, over a number of different time-scales or both. Initially, a series of sensor readings can be taken at the given sampling rate and a Fast Fourier Transform (FFT) performed on each: this is a form of short term averaging and is normally carried out because the target is thought to generate signals with a specific, unchanging frequency spectrum over the averaging period under consideration. This condition being satisfied, the FFT will highlight the target spectrum and thus improve the signal to noise (S/N) ratio, improving the identification process in terms of both target detection and frequency determination. The FFTs can then be averaged across the array of sensors, although if the precise sensor and target positions are unknown, this may only be carried out on the sensor powers, i.e., phase information is lost in such cases.

If further refinement is required, a series of FFTs on overlapped or subsequent sets of sensor readings can be taken. Of course, such a process is only really useful if coherent averages are taken. This is straightforward if the target remains stationary relative to the array and the mean array shape is unchanging with respect to the time-scales involved, so that the relevant frequency dependent phase corrections can be made: overlap averaging of this kind is quite commonly used for small arrays and can further improve the S/N ratio in the process of target detection and frequency determination, without additional knowledge of either the target position or the array shape. In both these time frames, target location can be performed with varying degrees of success according to the relative magnitude of the noise inputs to the system. Clearly, by preserving the correct phase information in the FFTs during overlap averaging the S/N ratio can be continuously improved with increasing numbers of overlaps provided that the target and mean array positions continue to remain in fixed relationships to each other. If they do not, some progress can nonetheless still be made if their relative motions can be estimated in some way.

This leads on to long term averaging where the target position and mean array shape are both assumed to alter, albeit slowly, with time and some form of weighted moving average of the results of target location are then used. In this time frame, target tracking and model evolution can be performed so that position estimate errors can be further diminished by using generalised knowledge about the behaviour of targets and their ability to manoeuvre within the given time frame [6] alongside hydrodynamic predictions of likely sensor motions. In this article all but the last of these methods of averaging will be investigated, i.e., up to and including overlapped FFTs with simple target modelling and weighted moving averages but without hydrodynamic predictions of sensor motions.

# 3 TARGET IDENTIFICATION

Before the locations of targets may be estimated it is, of course, necessary to identify any targets that may be present. For most purposes in sonar processing this means the identification of fixed frequency tones that lie above the noise floor of the signals being analysed. As has just been noted, this leads directly to the use of FFTs to produce power spectral density estimates for each sensor in an array. Then, if there are obvious spikes in the amplitudes of these spectra, a target is considered present. Target identification is thus intimately dependent on the noise level present in the spectra. In general, and as has already been mentioned, this can only be effectively controlled by averaging such spectra, preferably in a coherent fashion. If insufficient sensors or time slices are taken or the data are averaged incoherently (i.e., the phase information is ignored, probably because the sensor and target positions are not known with sufficient accuracy) quiet targets may well not be identified from the background noise. Of course, in the real world any target tone may also disappear or slowly change frequency or new tones may suddenly appear. Here, however, fixed tones that are present throughout the data sets will be used, although one of these will be below the noise floor that may be reached by incoherently averaging the sensor data.

By way of example, consider an array that is attempting to locate an unknown number of possibly low noise targets. The data collected by the sensors

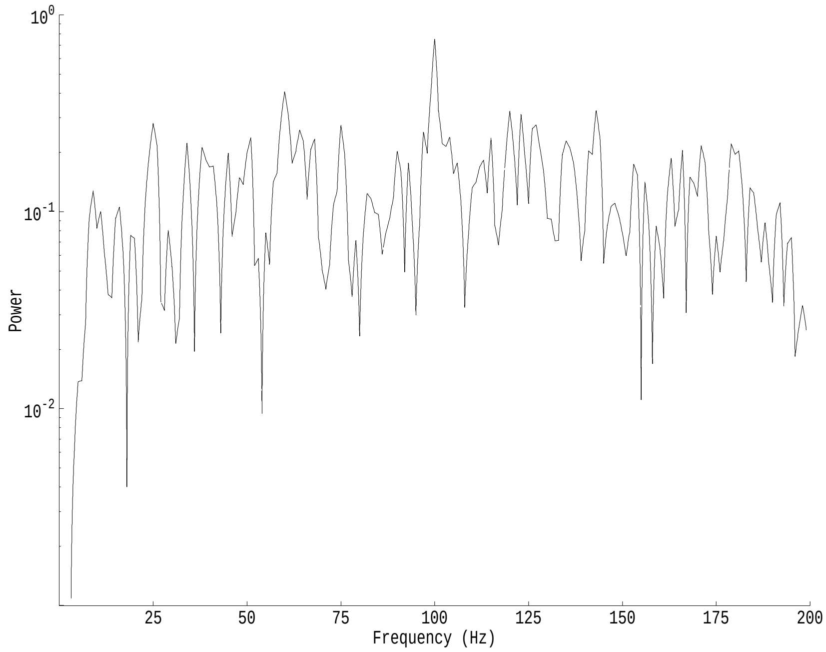


Figure 1: typical FFT from an individual sensor.

can then be written as

$$X(t) \;=\; [x_1(t), x_2(t), ...] \quad . \tag{1}$$

In order to filter out uncorrelated noise so as to distinguish targets, an FFT on a suitably windowed version of the data is performed first. Since the sampling rate for the data to be used here is set at 512 samples per second, the same number of data is chosen to perform the FFT, i.e., 512 data points are taken from each sensor simultaneously. In the frequency domain the data can be written as

$$Y(f) \;=\; [y_1(f), y_2(f), ...] \tag{2}$$

where $y_1(f)$ is the FFT of $x_1(t)$ from sensor one, and so on.

Now each $y(f)$ is an array of 512 elements, with real and imaginary parts for each individual frequency component, ranging from zero frequency upwards, with the first 256 values being unique. For a signal with poor signal to noise ratio, the FFT from a single sensor may not give a clear indication of the frequency spectrum of the target signal. If the range and bearing of the target are known alongside the positions of the sensors, then the signals at each sensor can be coherently added so as to enhance the spectral component (if this condition is not satisfied, the best that can be hoped for is a power addition of the spectral components). When the noise is uncorrelated, integrating the FFT

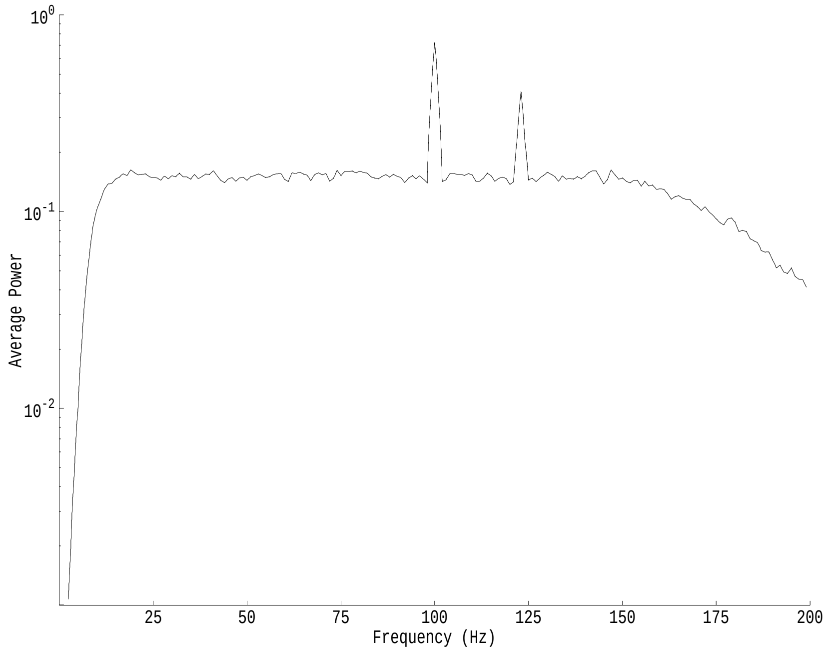


Figure 2: typical incoherently averaged FFT taken across an array of 225 sensors.

power output from all sensors will enhance the signal while in effect smoothing the random noise component, thus

$$Y_s(f) \;=\; \left|\sum_{m=1}^{M} y_m(f)\right| \tag{3}$$

where $M$ is the number of sensors. Further suppression of the noise may be sought by averaging the data over a number of time periods often employing some kind of overlap (commonly 50% overlaps are adopted when using Hanning (or von Hann) windows). Such overlap averaging can be carried out before or after averages are taken across the array. If they are taken before the spatial average and each individual sensor position is unchanging in its mean distance from the target during the overlaps (or the changes are known or estimated), the average can be carried out coherently and the S/N ratio further improved whether or not the spatial averaging is also carried out coherently. Figure 1 shows a typical FFT derived from an individual sensor using simulated data, while Figure 2 represents the incoherently averaged power signal taken across an array of 225 such sensors. Figure 3 shows a further spectrum, where 30 time slices of data (i.e., spanning a 30 second length of simulated record) have been coherently averaged together with 50% overlaps, followed by an incoherent spatial power average across the array, clearly demonstrating the improved S/N

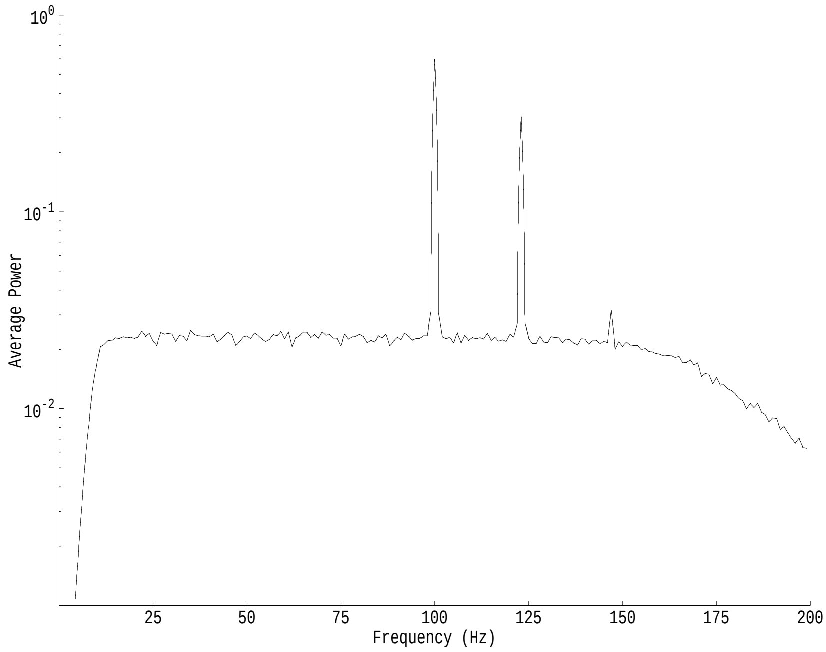


Figure 3: typical FFT where 30 time slices of data have been coherently averaged together with 50% overlaps, followed by an incoherent spatial power average across the array.

performance that may be obtained (of course, this S/N ratio can be improved still further by averaging coherently across the array elements but this requires knowledge of the relative positions of the target and the elements - the calculations behind Figure 3 only require the target to remain stationary with respect to the elements). In Figure 1 only one target can be clearly seen, in Figure 2 a second is apparent and in Figure 3 a third. These three signals are at 100 Hz, 123 Hz and 147 Hz, respectively and, relative to the signal at 100 Hz have levels of 0dB, -5dB and -25dB. The noise floor in the single, incoherently spatially averaged time slice is at -14dB, i.e., above the level of the third signal. Note that these plots are limited to 200 Hz so that they stay well below the Nyquist frequency, which is here 256 Hz.

# 4 TARGET LOCATION

Having identified the presence of one or more targets, most analytical techniques in target location then involve the solution of a set of simultaneous equations which generally require the manipulation of matrices. For small array dimensions this represents a reasonable overhead in terms of computational effort and memory requirement. However, as the array size increases this feature becomes

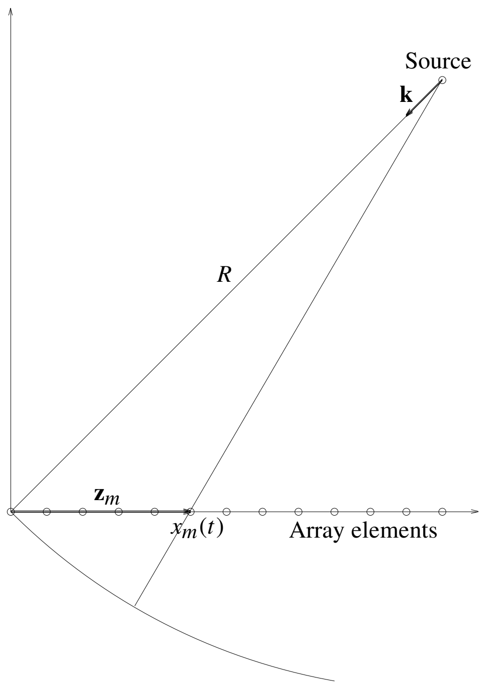


Figure 4: a spherical wave signal $s(t)$ propagating in a medium at speed $v$ from a source positioned in a direction $-\mathbf{k}$ from the first sensor of an array of $M$ sensors positioned at $\mathbf{z_m}$ and generating signals $x_m(t)$ in these sensors.

less acceptable as the costs in both computation and memory increase with the square of the number of elements. Thus for arrays of hundreds of elements or more, the prime consideration in such work is the tractability of the techniques involved. Additionally, a generalised approach is required that does not limit the solution to one dimension (i.e., bearing) but that can also deal with two- or three-dimensional problems, as is the case for a target in the near-field of a possibly non-linear passive sonar array. Numerical techniques have been used widely in various areas to solve problems which would be difficult or impossible by analytical methods and so attention is now turned to how well a passive sonar system consisting of a linear array of hydrophones, together with appropriate signal processing and numerical techniques can determine the range and bearing of individual targets.

When a spherical wave-front is used for beam forming, the so called array manifold varies along the array. Assume that a spherical wave signal $s(t)$ is propagating in a medium at speed $v$ from a source positioned in a direction $-\mathbf{k}$ (a unit vector) from the first sensor in the array, see Figure 4. An array of $M$ sensors is present in the medium: each one is assumed to record the acoustic field at its spatial position with perfect fidelity. The wave form measured at the $m$th sensor relative to that at the first is denoted by $x_m(t)$ and is given by

$$x_m(t) \;=\; s\left(t + \frac{R - |R\mathbf{k} + \mathbf{z_m}|}{\mathbf{v}}\right) + q_m(t) \tag{4}$$

where $\mathbf{z_m}$ is the position vector of the $m$th sensor measured from the first, and $q_m(t)$ is additive noise. This noise may be due to disturbances propagating in the medium or generated internally in the sensor or due to array element location uncertainty, etc.

One of the classical methods used in array processing for finding the bearing of an acoustic source is time delay beam-forming [19]: the outputs of the sensors are summed with weights and delays to form a beam, $B(t)$ where

$$B(t) \;=\; \sum_{m=1}^{M} a_m x_m(t - t_m) \quad . \tag{5}$$

The idea behind beam-forming is to align the propagation delays of a signal presumed to be propagating in a direction $\mathbf{k}$ so as to reinforce it. Signals propagating from other directions and also the noise are not reinforced. If the delay $t_m$ is ideally compensated by the signal delay $(R - |R\mathbf{k} + \mathbf{z_m}|)/\mathbf{v}$, the signal would be completely reinforced. The delayed output of each sensor would then be

$$x_m(t - t_m) \;=\; s(t) + q_m(t - t_m) \quad . \tag{6}$$

The resulting beam output becomes

$$B(t) \;=\; M s(t) + Q(t) \quad . \tag{7}$$

Thus the signal amplitude in $B(t)$ is $M$ times that measured at each sensor while the noise amplitude is increased by only $\sqrt{M}$ (assuming the noise outputs from the sensors are uncorrelated). Generally, the energy in the beam $B(t)$ is computed for many directions-of-look, $-\mathbf{k}$, by manipulating the delays $t_m$. Maxima of this energy, as a function of $\mathbf{k}$ are assumed to correspond to acoustic sources, and the source bearings correspond to the locations of these maxima. For a far field target, the interval between successive delays is constant for a linear array with uniform spacing between elements. For an array of length $D$, in the case of the example to be considered here 761.6m, the estimation of the boundary of the near-field zone of the array is at $2D^2/\lambda$ , or here approximately 77km at 100Hz. For a target at 100km with bearing 90.12° from the first element, the phase difference between the first and last elements is 107.9° at 100Hz (note that all bearings given in this article are absolute and based on a right handed axis system with true north at 0° and depth positive downwards). For a plane wave this phase difference would be 38.3°. This simple example demonstrates the inadequacies of the plane wave assumption in such cases.

If the target is in the near-field and the array sensors are no longer co-linear these ideas can still be used relatively easily. Assuming, for the moment, that the target bearing and range are known, the advancing curved phase front can be compensated for by modifying the phases seen at each sensor, depending on its location. Beam forming can then be carried out on the modified data. Here it is convenient to first average coherently across a set of $N$ overlapped time slices and then coherently across the $M$ elements. The amplitude in the beam at frequency $f$ is then

$$B_m(f) \;=\; \left| \sum_{m=1}^{M} \sum_{n=1}^{N} y_{mn}(f) \mathrm{e}^{\mathrm{i}(2\pi f n \delta t \;+\; \phi_m)} \right| \tag{8}$$

where $y_{mn}(f)$ is the Fourier transform of the $m$th sensor signal taken over time slice $n$, $\delta t$ is the interval between time slices and $\phi_m$ is a phase angle correction which allows for the positions of individual sensors relative to the first when compared to that of the target. This is given by

$$\phi_m \;=\; \frac{2\pi}{\lambda} \sqrt{(Rcos(\theta) - \Delta x_m)^2 \;+\; (Rsin(\theta) - \Delta y_m)^2} \tag{9}$$

where $R$ and $\theta$ are the assumed range and bearing of the target from the first sensor in the array and $\Delta x_m$ and $\Delta y_m$ are the coordinates of the $m$th sensor relative to the first one. Target location then requires the maximization of this signal by manipulation of $R$ and $\theta$, i.e., it becomes a two-dimensional search process.

If the target or array moves during the time overlaps used to improve the S/N ratios then estimates must be included to allow for the further phase shifts caused by these motions, i.e., $R$, $\theta$, $\Delta x_m$ and $\Delta y_m$, and hence $\phi_m$, all change with time slice $n$ [7]. The simplest model that can be proposed for such motions is to assume that $\mathrm{d}R/\mathrm{d}t = \dot{R}$ and $\mathrm{d}\theta/\mathrm{d}t = \dot{\theta}$ are constant and that $\Delta x_m$ and $\Delta y_m$ are known for each $n$, being taken from array instrumentation (notice also, that suitable choices of $\dot{R}$ and $\dot{\theta}$ will compensate for errors in the instrumentation data to some extent, since these errors can be thought of as being mapped into additional target motions which are then estimated by $\dot{R}$ and $\dot{\theta}$). It is, of course, also possible to model the target's course and speed along with those of the tow vessel and use these instead of $\dot{R}$ and $\dot{\theta}$ if it is thought that these will give more reliable estimates. If the values of $\dot{R}$ and $\dot{\theta}$ are not known *a priori*, as is usually the case, suitable values can be searched for, increasing the number of parameters to be considered from two to four. If it is further desired to

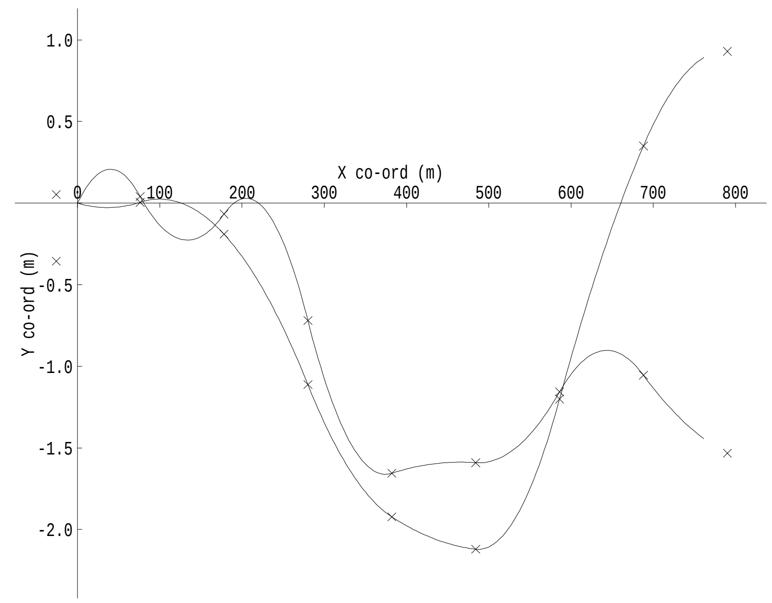


Figure 5: apparent compass locations ($\times$) and array shapes for two consecutive positions of an array in a simulated tow sequence separated by a one second interval.

acquire targets during such a process, the frequencies being dealt with can also be scanned, adding a fifth variable to be considered. As will be seen later, it is not practicable to investigate even a two-dimensional problem of this type using exhaustive search methods and thus the problem naturally becomes one of array power *optimization*.

# 5 ARRAY SHAPE UNCERTAINTY

As has just been noted, the ability to carry out coherent averages is dependent on knowledge of the array shape and how it changes with time. The effects of array element position uncertainty can thus be considered as a further noise input, e.g., treating the distorted array as a linear equally spaced array, the phase front will reflect both the signal delay and the displacement of the array elements.

A considerable amount of work has been undertaken in the field of antenna behaviour on the effect of random and systematic errors in the radiation pattern of the antennas. This work can be directly applied to the case of sonar arrays of uncertain shape. Simplistically, the problem can be addressed in terms of the order of the mean shape of the array. This shape can be described in general terms by a polynomial expansion consisting of linear, quadratic, and higher terms. It is relatively easily seen that a systematic linear phase error down the length of the array is essentially a heading error and simply maps into a bearing error in any target location algorithm. On the other hand, a quadratic component is in effect superimposed on any spherical wave-front that may impinge on the array. This error therefore contributes to an increase (or decrease) in the apparent curvature of the wave-front and hence effectively yields an error in range estimation. Higher order errors generally have major effect in bearing for odd powers and range for even powers. If the array shape can be estimated, however, suitable steps can be taken during the beam forming process to allow for these effects. Moreover, when the array is curved, it is often possible to resolve target bearings without the spatial ambiguity inherent in processing the data from straight arrays.

# 6 ARRAY SHAPE MODELLING

Because of the problems inherent in processing data when the sensor positions are unknown, it is normal when building long flexible arrays to incorporate shape estimation instrumentation within the array [16]. Typically, compasses are positioned along the array and these may then be used to estimate its shape at any instant. Of course, such compass data is never precisely accurate and noise in this data must also be considered. Here, it will be assumed that a number of compasses are available and that they may be used to help in processing data from the array. To do this a curve fit is applied to the compass data such that the fitted curve has the correct slopes (i.e., bearings) at the compass positions and the correct arc lengths between them. This is most readily achieved by simply fitting independent arcs of circles between each compass that meet tangentially at the compass positions (and which are then independent of the axis system in use). The hydrophones positions can then be readily calculated from the assumed shape. Figure 5 shows the apparent compass locations and array shapes for two consecutive positions of an array in a simulated tow sequence separated by a one second interval. In both cases the array is, in fact, straight and compass errors account for the deviations from this. It can be seen that the compass data changes sufficiently from time slice to time slice for a detectable change in the fitted shape to occur, but that the change is small compared to the array's overall length (note the difference in axis scales).

# 7 EXAMPLE DATA

Having outlined the background to this problem and suggested how target detection and positioning might be carried out, these ideas are next applied to a set of simulated data. This set consists of 225 individual sensor outputs, each sampled at 512 readings per second for a period of 1,400 seconds, plus nine compass outputs read every second (the simulation therefore contains over 160 million individual items of data). During the run there are two targets present. Target one emits two tones: the first at 100 Hz and 0dB and the second at 123 Hz and -5dB. The second target emits a single tone of 147Hz at -25dB. The background noise level is at -14dB, i.e., as per the previously discussed spectra. At all times during the run the targets remain at fixed (absolute) bearings and distances from the ship towing the array: target one is at $90°$ and 100km (i.e., due east) and target two at $180°$ and 100km (due south). To begin with all three vessels are travelling south (i.e., on a course of $180°$) at 10 knots, then after 600 seconds all ships execute a turn on to a course of $270°$ (west). Thus, since the array streams out behind the tow ship, the array begins broadside-on to target one and end-on to target two and then, as the turn is carried out, this reverses: the array becomes end-on to target one and broadside to target two, see Figure 6. Note that since the first hydrophone in the array lies 204.43m behind the datum used for positioning the ships, its target bearings and ranges in the subsequent analysis are slightly different from those for the datum and, moreover, change slightly as the ships change course despite the ships maintaining fixed stations to each other.

# 8 SIMPLE TARGET LOCATION SEARCHES

To begin with, a number of simple target location searches will be discussed which illustrate the basic performance of the algorithm being suggested. Subsequent sections then examine the use of a modern stochastic search method when applied to this problem. Throughout these searches it is assumed that the three target tones present in the example data have already been identified and so frequency searches are not considered. Of course, if this were not the case this additional variable would also have to be scanned.

## 8.1 Noise-free data - linear array

The most basic kind of search that can be proposed simply involves dividing the target space into a large number of search areas and then coherently summing the array powers from a single time slice across all 225 hydrophones at the corners of each search area. For convenience, the space can be divided up in cylindrical coordinates, with the angle varying from $0°$ to $180°$ (given the left/right ambiguity inherent in a linear array) and $R$ from 0 to the boundary of the search space to be covered. Table 1 contains the results of a number of such searches when applied to the first tone of target one (100Hz) with a set of noise free target data while the array is straight and broadside-on to the

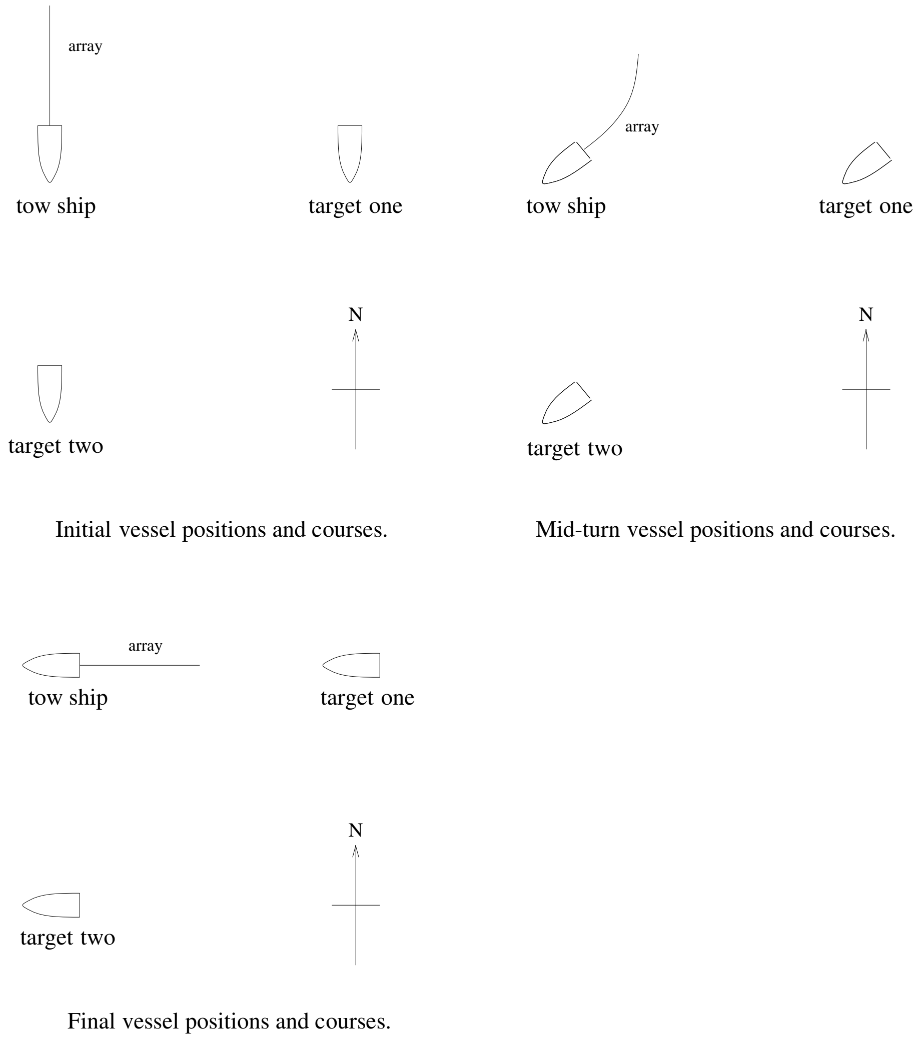


Figure 6: tow ship, array and target manoeuvres during the example data set.

| Bearing step size | Range step size | Bearing ($\theta$) | Range ($R$) |
|---|---|---|---|
| (degs) | (m) | (degs) | (m) |
| 0.0001 | 10 | 90.1172 | 100,010 |
| 0.001 | 10 | 90.117 | 99,510 |
| 0.01 | 10 | 90.12 | 101,910 |
| 0.0001 | 100 | 90.1172 | 100,100 |
| 0.001 | 100 | 90.117 | 99,450 |
| 0.01 | 100 | 90.12 | 102,000 |
| 0.001 | 1,000 | 90.117 | 99,000 |
| 0.1 | 10,000 | 90.1 | 70,000 |

Table 1: bearing and range results for various simple search step sizes, linear array, noise-free data.

target. In this condition the actual range and bearing of the target from the first hydrophone (the datum used here) are 90.1172° and 100.0 km. It is apparent that the step size in $\theta$ plays a more important role than that in $R$. This is due to the relatively slow variation of array gain with angle compared with that in range. Typically, to achieve 10m accuracy for a target at 100km, a step size of 0.0001° in bearing is needed. If a space of 0° to 180° and range from 0 to 150km is being investigated with such detailed step sizes, several hours are needed to complete an exhaustive search. Therefore, to minimize the computational effort involved, large step sizes can be chosen to perform a coarse search, followed by a reduction in step sizes with searches concentrated in the limited areas identified by the first search.

Thus to begin with, if a step size of 0.1° is chosen for the bearing and 10 km for range, maximum array power is found at 90.1° and 70km. A second iteration can then be limited to the area surrounding this point, but noting that a significant variation in range is still likely. If 0.001° and 100m are then chosen as steps the maximum power is found at 90.117° and 99.45 km. A third iteration with steps of 0.0001° and 10m then yields a target at 90.1172° and 100.010 km. Clearly, in the absence of noise, a simple power maximization technique can give a very accurate bearing and range estimation provided the search is carried out with sufficient resolution. Figure 7 shows a contour plot of the signal power corresponding to this target, illustrating how rapid the variation in power is with bearing.

## 8.2 Noise-contaminated data - linear array - fixed target positions

When there is noise appearing at the same frequency as the signal, the wavefront is no longer obviously spherical. Figure 8 shows typical phase fronts for

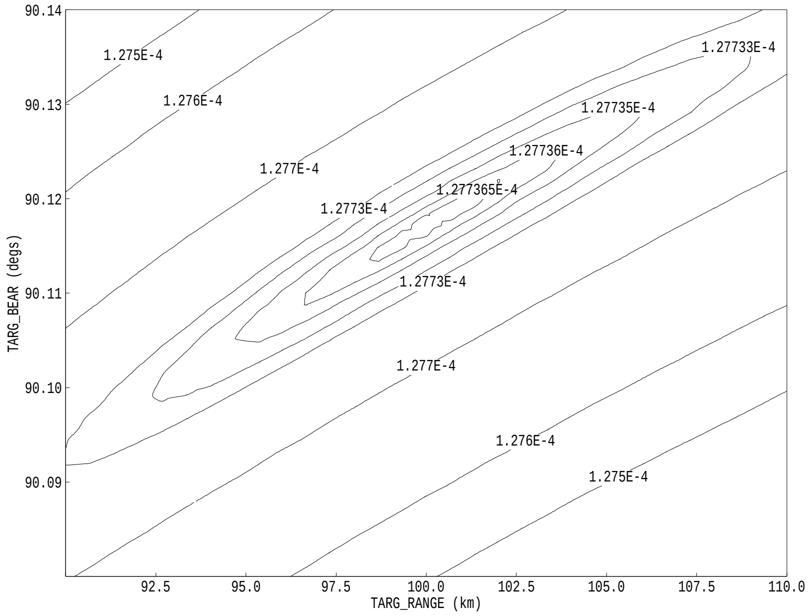


Figure 7: contour plot of signal strength for the 100 Hz tone of the first target in the vicinity of the target.

the two tones from the first target using a single set of 225 FFT readings which are distorted by background noise. Figure 9 shows how these phase fronts can be improved by using 30 sets of 50% coherently overlapped FFTs to smooth the data. With such distorted phase fronts it would be difficult to achieve great accuracy using traditional high performance analytical algorithms, because the assumptions behind these algorithms are no longer valid. Conversely, using the simple three stage search method with the power maximization technique adopted for the noise free data, the bearing errors on the broadside target can be controlled to around $0.5°$ with a range error of a few kilometres while the quiet target, end-on to the array, can be located to within $2°$ in bearing but, of course, only poorly in range (which theoretically cannot be resolved at all in the end-on case), see table 2. Notice that, since the targets are at the edge of the near-field zone for the array used here, the errors seen in the broadside target ranges are, in reality, as small as can be reasonably expected.

# 9 IMPROVED SEARCH ALGORITHMS

Having established the basic performance of the proposed power maximization method, attention is next turned to using a modern stochastic search method to speed up the target location process. Up until this point a three stage search has

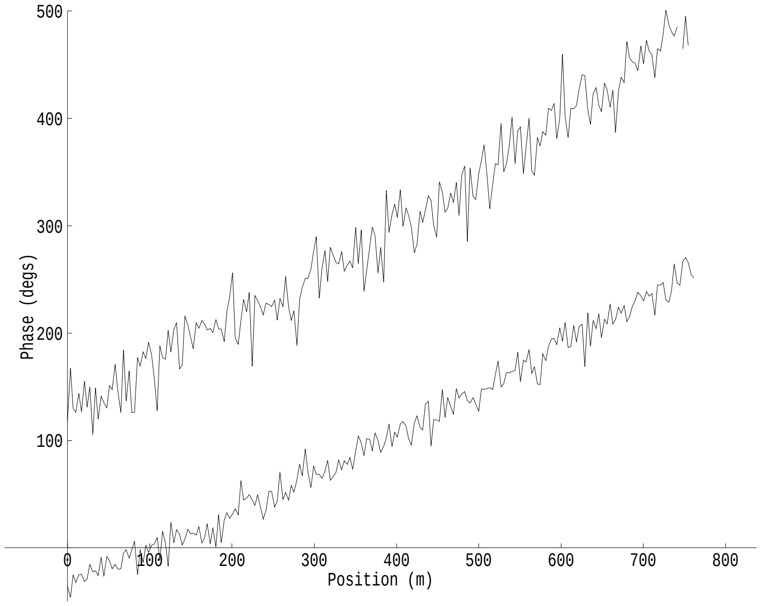


Figure 8: typical phase fronts for the two tones from the first target when distorted by background noise, using a single set of 225 FFT readings.

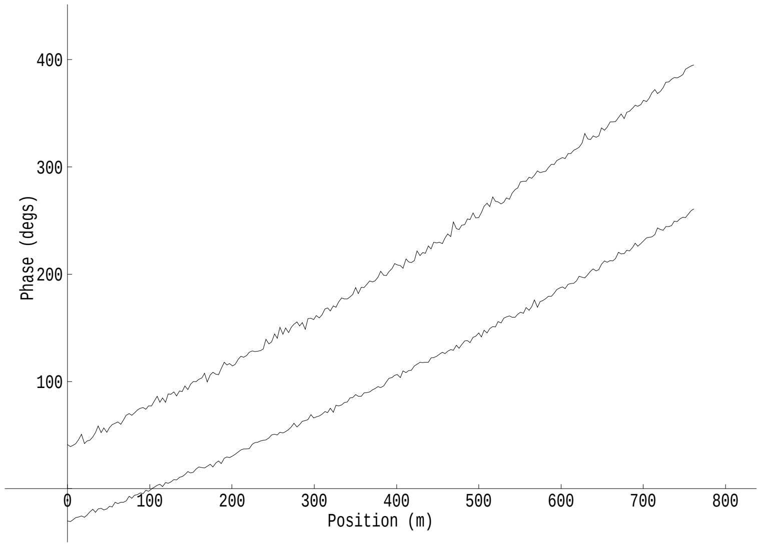


Figure 9: typical phase fronts for the two tones from the first target improved by using 30 sets of 50% coherently overlapped FFTs to smooth the data.

| Target freq. | True Bearing ($\theta$) | True Range ($R$) | Est. bearing | Est. range |
|---|---|---|---|---|
| (Hz) | (degs) | (m) | (degs) | (m) |
| 100 | 90.117 | 100,000.0 | 90.68 | 96,817 |
| 123 | 90.117 | 100,000.0 | 90.70 | 106,411 |
| 147 | 180.0 | 100,204.4 | 178.48 | 4,459 |

Table 2: bearing and range results for three target tones, linear array, noise-contaminated data, fixed target positions, exhaustive search.

been used that requires 20,000 locations to be examined at each stage to ensure complete accuracy in finding the targets. Such fine meshes are required because of the great sensitivity of the array to bearing changes. The problem posed here is, however, at most only a four dimensional search and thus amenable to optimization methods.

Genetic Algorithm (GA) methods can be used to carry out such searches and much recent research has shown that they are very robust when dealing with noisy or multi-modal problems [13], [14]. They work by maintaining a pool or population of competing estimates which are combined to find improved solutions. In their basic form, each member of the population is represented by a binary string that encodes the variables characterizing the solution. The search progresses by manipulating the strings in the pool to provide new generations of estimates, hopefully with better properties on average than their predecessors. The processes that are used to seek these improved designs are set-up to mimic those of natural selection: hence the method's name. The most commonly used operations are currently: (i) selection according to fitness, i.e., the most promising solutions are given a bigger share of the next generation; (ii) crossover, where portions of two good solutions, chosen at random, are used to form a new estimate, i.e., two parents 'breed' an 'offspring'; (iii) inversion, whereby the genetic encoding of a solution is modified so that subsequent crossover operations affect different aspects of the estimate and (iv) mutation, where small but random changes are arbitrarily introduced into an estimate. In addition, the number of generations and their sizes must be chosen, as must a method for dealing with constraints (usually by application of a penalty function).

The algorithm used here works with up to sixteen bit binary encoding (although parameters that are selected from a number of fixed possibilities use only the minimum necessary number of bits and the number of bits can be reduced by the user for continuous variables). It uses an elitist survival strategy which ensures that the best of each generation always enters the next generation and has optional niche forming to prevent dominance by a few moderately successful designs preventing wide ranging searches. Two penalty functions are available. The main parameters used to control the method may be summarized as:

1. $N_{\text{gen}}$ the number of generations allowed (default 10);

2. $N_{\text{pop}}$ the population size or number of trials used per generation which is therefore inversely related to the number of generations given a fixed number of trials in total (default 100);

3. P[best] the proportion of the population that survive to the next generation (default 0.8);

4. P[cross] the proportion of the surviving population that are allowed to breed (default 0.8);

5. P[invert] the proportion of this population that have their genetic material re-ordered (default 0.5);

6. P[mutation] the proportion of the new generation's genetic material that is randomly changed (default 0.005);

7. a Proportionality Flag which selects whether the new generation is biased in favour of the most successful members of the previous generation or alternatively if all P[best] survivors are propagated equally (default TRUE) and

8. the Penalty Function choice.

Using a method that incorporates these ideas the following GA based approach can be proposed for the problem of interest here: (i) maximize the array power by searching one half of the bearing space and the range values of interest using a GA search of 10 generations each of 250 evaluations with 12 bit resolution in both variables (i.e., use 2,500 points); (ii) reduce the bearing scan to $\pm 5^\circ$ around the best target found while leaving the range scan as before and search with 10 generations each of 100 evaluations (i.e., another 1,000 steps); (iii) reduce the bearing scan further to $\pm 0.25^\circ$ and the range scan to $\pm 25$km around the best target and carry out a final GA search of 10 generations each of 100 members and with increased resolution of 16 bits (i.e., 1,000 points); (iv) finally, if left-right ambiguity must be resolved repeat this process starting in the other half of the bearing search space.

This search uses only 4,500 points and is able to robustly locate the same results as the previous exhaustive search process, taking a small fraction of the time (the three stage exhaustive search examines 20,000 points). It is worth noting, however, that an exhaustive search is the only way of guaranteeing that all targets have been found to within a given resolution. Therefore, if time permits, it is still to be preferred over other methods. Lastly, it should be noted that search tasks like this can often be handled by parallel processing devices, something the GA is particularly well suited to.

| Target freq. | True Bearing ($\theta$) | True Range ($R$) | Est. bearing | Est. range |
|---|---|---|---|---|
| (Hz) | (degs) | (m) | (degs) | (m) |
| 100 | 90.117 | 100,000.0 | 90.35 | 38,198 |
| 123 | 90.117 | 100,000.0 | 90.58 | 70,485 |
| 147 | 180.0 | 100,204.4 | 177.07 | 3,963 |

Table 3: bearing and range results for three target tones, *noisy compass readings*, noise-contaminated data, fixed target positions, GA search.

### 9.1 Noise-contaminated data - array position inaccuracy - fixed target positions

When towing an array of the length considered here, even if the tow ship maintains a steady course, the array will fluctuate in shape. This much has been noted already and a method proposed whereby compass data can be used to provide an estimate of the array shape. Therefore, consideration is next turned to the effects of these uncertainties on the ability of the array to locate targets using the method proposed. Table 3 repeats the results presented in table 2 but now using sensor positions based on the compass data (rather than the true positions used for table 2) along with estimated values of $\dot{R}$ and $\dot{\theta}$ (since although the targets maintain fixed positions, suitable values of these parameters help correct for errors in the array shape estimates). Here, the compass readouts have been set to have random fluctuations of up to $\pm 2°$ and these give rise to the estimated array shapes such as those already shown in Figure 5. As can be seen from the table, the bearings are still accurate to within $0.5°$ for the two more powerful tones and to within $3.0°$ for the low noise one. However, the shape errors have significantly degraded the accuracy of the broadside target ranges, which are now predicted only to within a factor of about 2.5. Nonetheless, it should be stressed that since the targets are at the edge of the near-field zone of the array and now the array suffers from position errors, which are known to significantly affect range accuracy, these values are still quite respectable. As will be seen later, by taking a moving average of the target range with time, these range estimates can be further improved upon. It is also worth noting that, when the array is broadside-on to the quiet target, it can also be resolved to within $\pm 0.5°$ in bearing and a factor of about 3.0 in range.

### 9.2 Noise-contaminated data - array position inaccuracy - curved array - moving targets

Lastly within this section, attention is turned to the location of targets when the tow and target vessels turn. This leads to significant changes in the array shape which can only be easily deduced from the compass data, i.e., equation (9) can

| Target freq. | True Bearing ($\theta$) | True Range ($R$) | Est. bearing | Est. range |
|---|---|---|---|---|
| (Hz) | (degs) | (m) | (degs) | (m) |
| 100 | 90.04 | 99,808.0 | 90.31 | 69,965 |
| 123 | 90.04 | 99,808.0 | 87.55 | 241,406 |
| 147 | 180.11 | 100,070.1 | 183.62 | 252,589 |

Table 4: bearing and range results for three target tones, curved array, noisy compass readings, noise-contaminated data, *moving targets*, GA search.

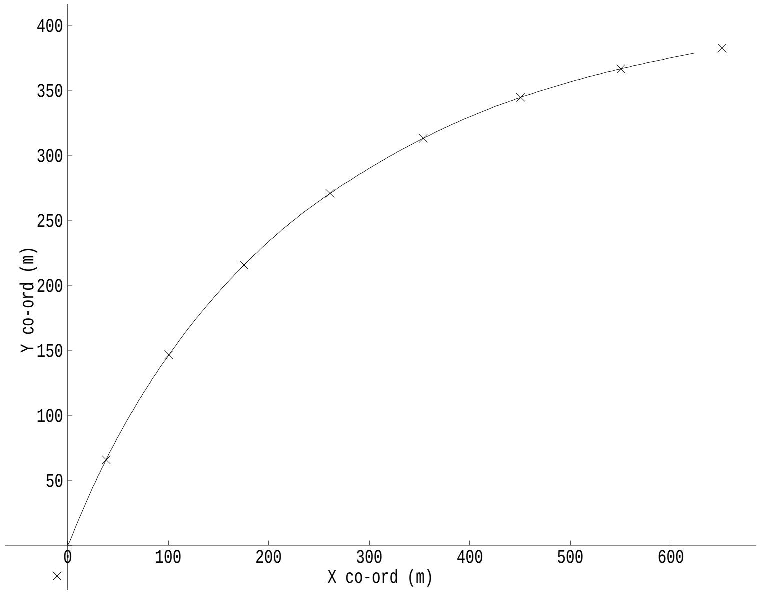


Figure 10: apparent compass locations ($\times$) and array shape during the turn.

only be used if some estimate of the array curvature is made (of course, given suitable hydrodynamic modelling these estimates might be improved). Moreover, during the period used for averaging, the target ranges and bearings alter slightly in this case. Although these changes are only small, those in bearing are sufficient to affect the location process. Table 4 gives the equivalent results to those presented in tables 2 and 3 but now with the sensor positions based on the compass data *during the turn* and again using estimates of $\dot{R}$ and $\dot{\theta}$ alongside those of $R$ and $\theta$. Here the compass data give rise to estimated array shapes such as that shown in Figure 10 and substantial curvature is clearly present. As can be seen from the table the target bearings are predicted with nearly as great an accuracy as those for the straight array. Moreover, the range estimates for all three target tones are now of similar quality, all remaining within a factor of about 2.5 of the true values. This is as expected, since, during the turn, the array is not end-on or broadside-on to either of the targets. Again, as has been noted in the previous sub-section, moving averages of target positions further improve these results. Finally, it should be noted that the four variable search/power optimization problem being solved here is by no means trivial. As will be seen in the next section, attempts to locate the targets using classical, slope ascent methods [23] consistently fail to find adequate solutions. No doubt this is due to the extreme sensitivity of the array power to the bearing selection and also the noisy nature of the data (which means that the function being optimized is not uni-modal or smooth). This difficulty is further compounded by trying to find suitable choices of $\dot{R}$ and $\dot{\theta}$.

# 10 OTHER SEARCH METHODS

Before going on to look at the ability of the proposed GA search method to track targets over extended periods of time it is worth considering whether or not other optimization methods might also be useful in this context. Optimization techniques have been studied for very many years and over that time a considerable number of methods have been proposed. A number of authors have collated these methods into libraries allowing comparison to be made between them [23], [22], [12]; the last of these libraries, called OPTIONS, is used here. This library contains, in addition to the GA, the following methods:

- adaptive random search (Adrans) [23];
- Davidon, Fletcher, Powell strategy (David) [23];
- Fletcher's 1972 method (Fletch) [23];
- Jacobson and Oksman method (Jo) [23];
- Powell's direct search method (PDS) [23];
- Hooke and Jeeves direct search as implemented by Siddall (Seek) [23];
- the simplex strategy of Nelder and Meade as implemented by Siddall (Simplx) [17], [23];
- the method of successive linear approximation (Approx) [23];
- random exploration with shrinkage (Random) [23];
- NAg routine E04UCF, a sequential quadratic programming method (NAg) [5];
- a Bit Climbing algorithm (BClimb) [4];

- a Dynamic Hill Climbing algorithm (DHClimb) [25];
- a Population Based Incremental Learning algorithm (PBIL) [2];
- the routine POWELL taken from the Numerical Recipes cookbook (NumRcp) [20];
- repeated application of a one-dimensional Fibonacci search (FIBO) [22];
- repeated application of a one-dimensional Golden section search (Golden) [22];
- repeated application of a one-dimensional Lagrangian interpolation search (LAGR) [22];
- Hooke and Jeeves direct search as implemented by Schwefel (HandJ) [22];
- Rosenbrock's rotating co-ordinate search (ROSE) [21], [22];
- the strategy of Davies, Swann and Campey with Gram-Schmidt orthogonalization (DSCG) [22];
- the strategy of Davies, Swann and Campey with Palmer orthogonalization (DSCP) [22];
- Powell's strategy of conjugate directions (Powell) [22];
- the Davidon, Fletcher, Powell strategy (DFPS) [22];
- the simplex strategy of Nelder and Meade as implemented by Schwefel (Simplex) [17], [22];
- the complex strategy of Box (Complex) [3], [22];
- Schwefel's two-membered evolution strategy (2MES) [22];
- Schwefel's multi-membered evolution strategy (MMES) [22];
- Simulated Annealing (SA) [15];
- Evolutionary Programming (EP) [8] and
- an evolution Strategy based on the earlier work of Back, Hoffmeister and Schwefel (ES) [1].

Notice that several of the classical methods provided here are common although details of their exact implementations differ. They do not, therefore, always deliver the same results.

To assess the performance of the methods on the basic target location task, each technique has been used to scan the half-space to one side of the array

| Method | Overall Average | | | Method | Overall Average | | |
|---|---|---|---|---|---|---|---|
| | % sgth | % std dev | steps | | % sgth | % std dev | steps |
| Adrans | 85 | 27 | 9153 | David | 13 | 12 | 305 |
| Fletch | 14 | 12 | 180 | Jo | 13 | 14 | 49 |
| PDS | 25 | 31 | 891 | Seek | 36 | 38 | 3042 |
| Simplx | 22 | 27 | 229 | Approx | 15 | 14 | 360 |
| Random | 38 | 31 | 7844 | NAg | 10 | 10 | 24 |
| BClimb | 75 | 28 | 2500 | DHClimb | 87 | 13 | 2578 |
| PBIL | 78 | 15 | 2500 | NumRcp | 22 | 29 | 478 |
| FIBO | 71 | 33 | 1565 | Golden | 71 | 33 | 1619 |
| LAGR | 72 | 29 | 544 | HandJ | 81 | 29 | 2134 |
| ROSE | 14 | 12 | 2225 | DSCG | 46 | 34 | 235 |
| DSCP | 45 | 33 | 272 | Powell | 15 | 14 | 1151 |
| DFPS | 8 | 8 | 20 | Simplex | 59 | 32 | 2494 |
| Complex | 15 | 11 | 78 | 2MES | 65 | 28 | 235 |
| MMES | 29 | 33 | 2478 | GA | 86 | 11 | 2500 |
| SA | 81 | 13 | 2500 | EP | 86 | 10 | 2500 |
| ES | 78 | 12 | 2500 | | | | |

Table 5: comparative performance of methods across all three signals, coarse search, straight and curved array, coherent and incoherent noise; stochastic methods averaged over five runs.

looking from 5 to 200 km and at the three frequencies of the known signals for the model used. These searches have been carried out at 10 different time slices of the data for the uncorrelated background noise model (five when the tow ship is not turning and five when it is) and five when the noise is spherically correlated (and when the ship is not turning). This range of tests gives an understanding of the robustness of the methods (those for the modern stochastic methods have also been averaged over five different random number sequences). The corresponding results are presented in table 5. In all cases the optimizers were allocated a single pass of 2,500 trials for these searches (in many cases the search methods use this figure for guidance only and may take considerably more or fewer steps, depending on the algorithm in use).

It is apparent from the table that the most reliable methods for locating targets in a broad search area and with varying signal strengths, array shapes and noise models are stochastic in nature, with Dynamic Hill Climbing (DHC), the Genetic Algorithm (GA) and Evolutionary Programming (EP) performing best. Of these the GA and EP (a close relative) have the lowest standard deviations in their results and so are preferred over DHC (which just uses a series of random start points followed by a simple hill climber, and which explains its slightly more varied performance).

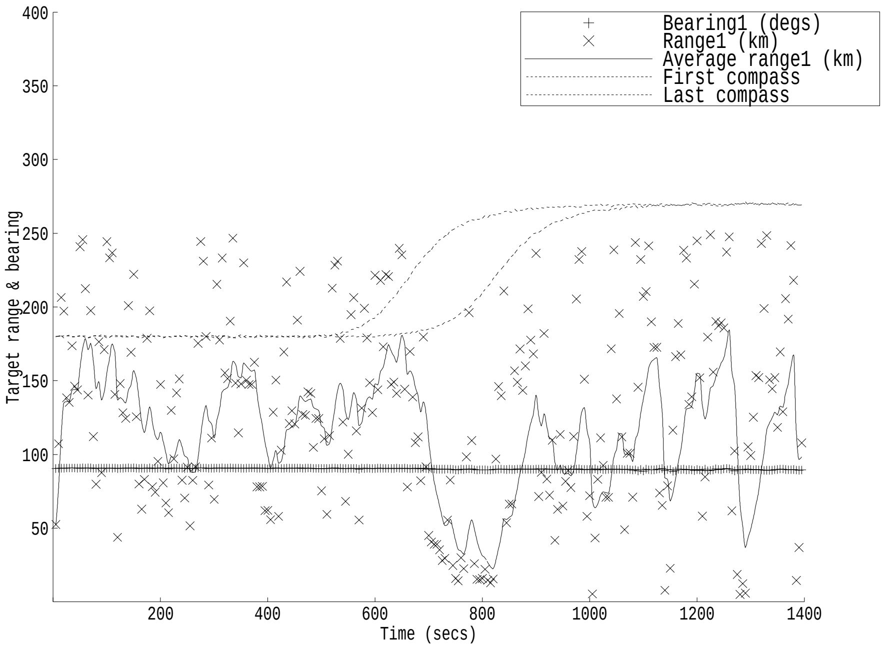


Figure 11: bearing and range tracks with moving range average, true targets; (a - tone one of target one).

Of the classical methods tried the performance of the Schwefel implementations of the Hooke and Jeeves search and the repeated one-dimensional searches (Golden Section, Fibonacci and Lagrange Interpolation) clearly performed best. A more detailed examination of the results than space allows here reveals that the Hooke and Jeeves method deteriorates as the signal being searched for becomes weaker. It also shows that the one-dimensional methods are less affected by this problem but they are clearly are not as robust as the stochastic methods. Such analysis also makes clear that it is much easier for most of the search mechanisms to locate targets when the array is straight.

# 11 TARGET TRACKING

Finally, the multi-pass GA optimization approach proposed here has been applied to the complete data set and the results used to track the three target signals over time, allowing moving averages of the ranges to be taken. Of course, when tracking targets that have already been located there is no need to search the entire range and bearing space at each time step. It is usually sufficient to use a slightly broader, one stage GA search in an area around the previously lo-

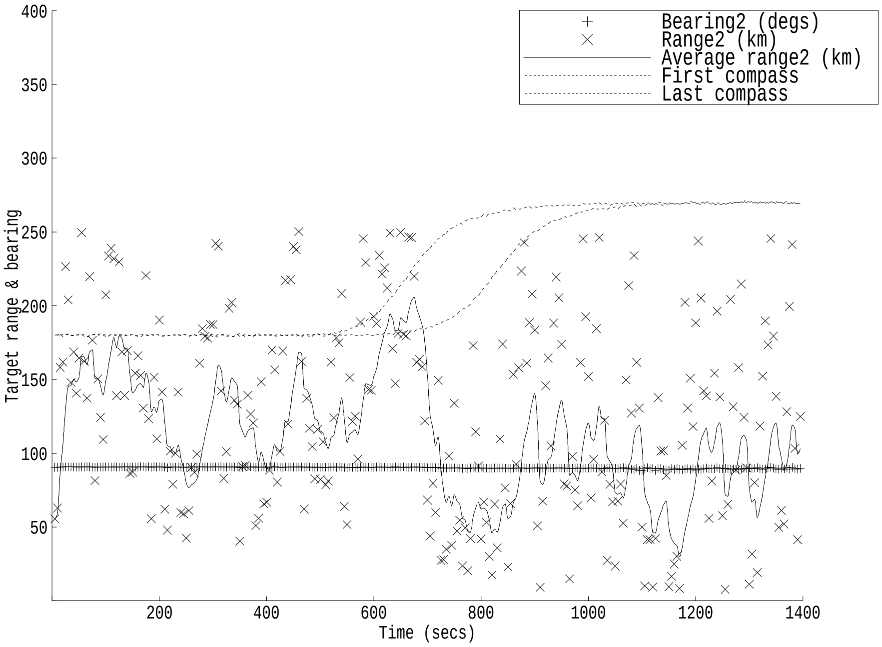


(b - tone two of target one).

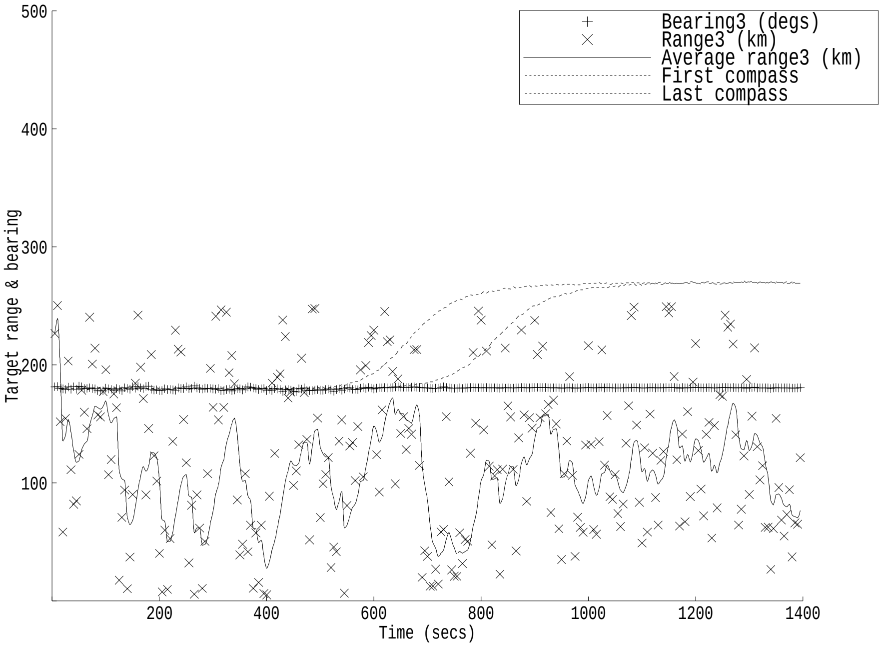


(c - tone one of target two).

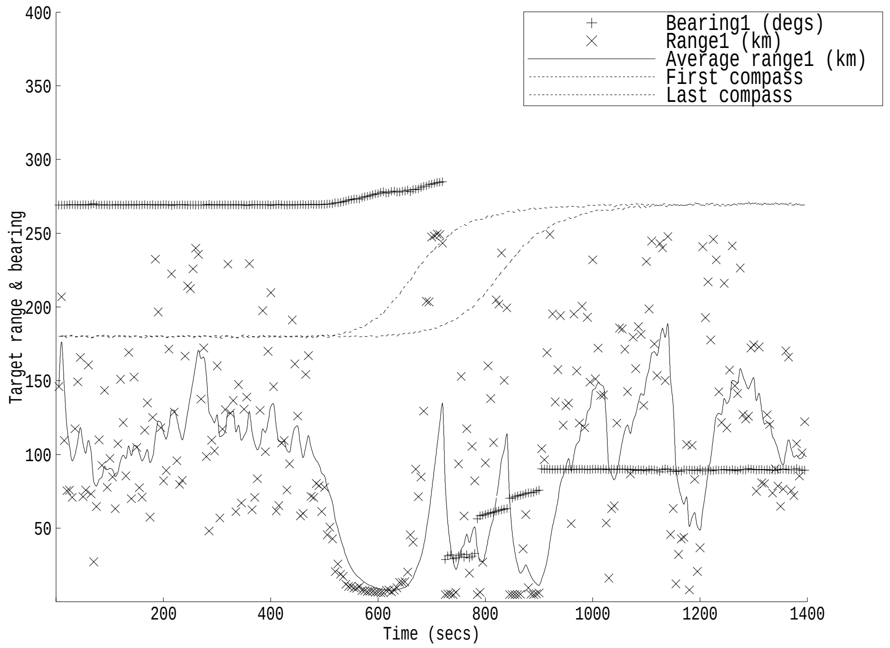


Figure 12: bearing and range tracks with moving range average, false targets; (a - tone one of target one).

cated positions, occasionally supplemented by the full three stage search. Here, the one stage search examines $\pm 0.5^{\circ}$ in bearing and $\pm 100$ km in range with 2,000 evaluations spread over 10 generations of the GA. These searches are carried out for every five seconds of data using five second time slices so that each new optimization uses fresh data. These are then updated by a full three stage search after every 60 seconds of data has been read. Here, both left and right hand signals have been tracked since, when the array becomes curved, the true targets should remain stationary while the false ones veer off and their power levels drop. The results of these searches are shown in Figures 11a-c and 12a-c where not only have the located maxima been plotted, but also exponentially time weighted geometric averages of the ranges (using a time constant of 30 seconds). Also shown on these plots are the compass readings from the compasses at either end of the array, which indicate the extent of the array curvature and the duration of the turn. Figure 13 then shows the power levels of the six tracked signals (and repeats the compass data for convenience): notice that when broadside-on to the array, the power traces are less smooth than when end-on, as might be expected, since the phase changes along the array in such cases are then significantly smaller, making the location process less precise. It is clear from these figures that the false targets can be readily distinguished

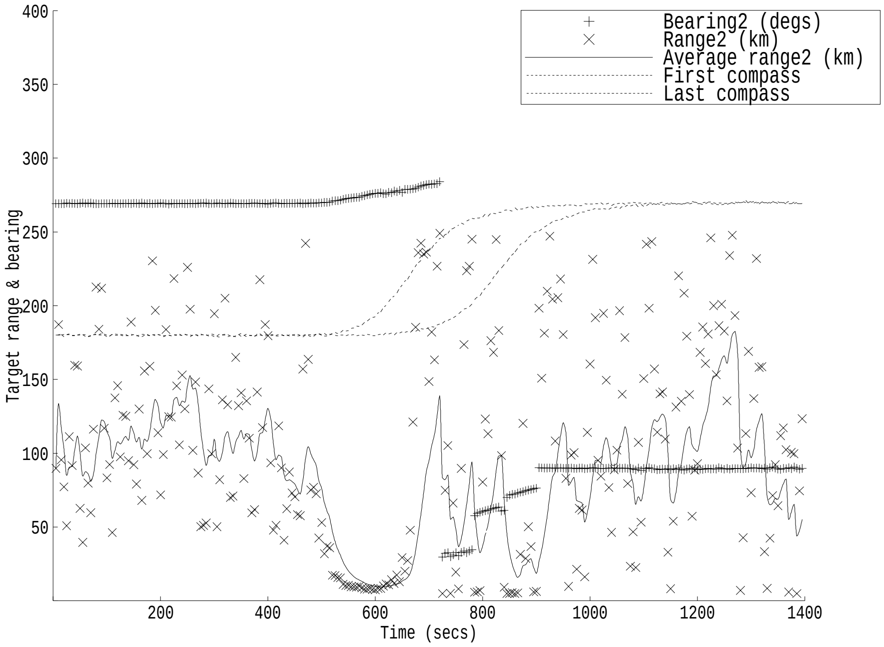


(b - tone two of target one).

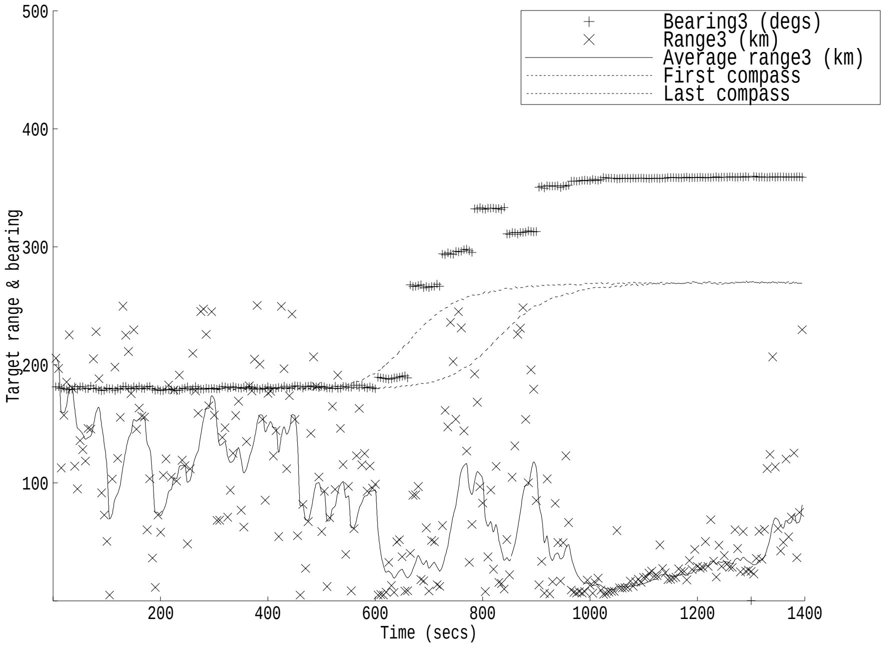


(c - tone one of target two).

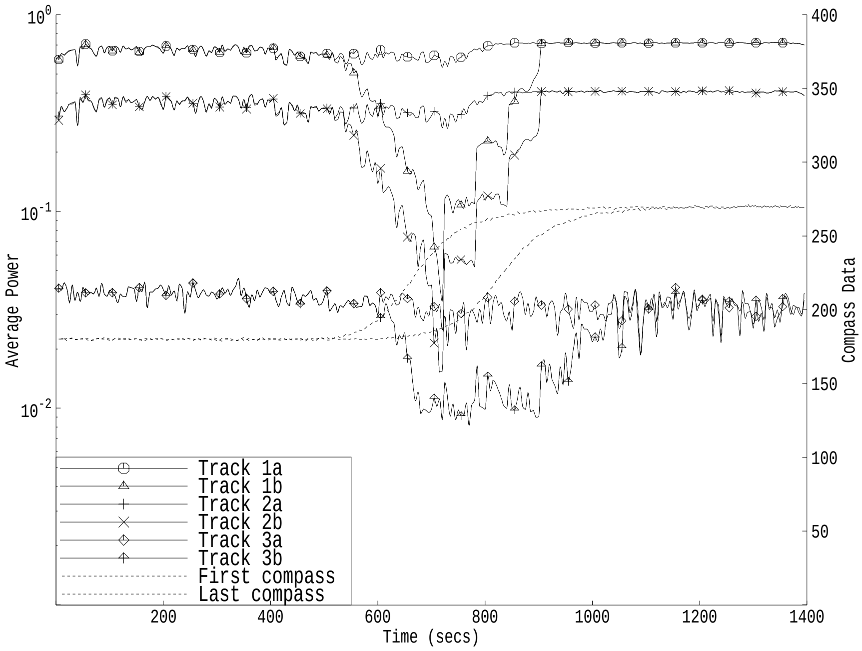


Figure 13: power levels of the six tracked signals; also showing first and last compass readings.

from the true ones when the array becomes curved: the false target bearings veer as the array changes shape; moreover, the power levels for the false targets are then lower than for the true ones (the steps in the traces occur when the full three stage GA searches relocate the rapidly veering false targets). It can also be seen that, when dealing with data corrupted by noise and when the array position is not known precisely, the true target ranges are rather oscillatory, while their bearings and power levels remain virtually stationary: hence the need for weighted moving averages to smooth the range data.

Overall, it is clearly possible to locate and track all three target tones during a course change when the array has considerable curvature. Moreover, it is also possible to resolve the left/right ambiguity inherent in the signals received by a linear array, by noting the bearing changes and lower powers of the false targets when the array becomes curved. In addition, the target bearing accuracies are of a high standard throughout while those for range are acceptable, especially given the fact that the targets lie at the edge of the near-field zone of the array and that the array is also subject to shape uncertainties.

## 12 CONCLUSIONS

A numerical technique for bearing and range searching in the near-field for large aperture passive sonar arrays has been presented. The technique gives precise location of targets with noise free data, and still performs well when the data is corrupted by noise. It is based on a simple power maximization approach but one that is corrected for target ranges as well as bearings and also allows for array shape changes. The array shapes are estimated using array compass data and further corrections are made by allowing for range and bearing shifts that occur while taking coherently overlapped FFT averages in the time domain. It is emphasized that, although the target identification work presented here has been carried out using simpler methods (since these are faster when it is known that the targets are stationary with respect to the array), the power maximization technique developed is fully capable of identifying targets even when they are moving and the array is curved in shape.

This work has established that reasonable target and bearing estimates can be obtained for very long arrays working with targets which are of the order of hundreds of kilometres from the array and lie at the edge of its near-field. The approach used lends itself to generalised optimization and search methods without incurring significant computational overheads and the use of a Genetic Algorithm has been shown to allow rapid range and bearing solutions to be obtained. The approach also allows for target track modelling so that moving averages can be obtained which allow improved range estimates to be obtained. Finally, it is worth noting that further refinements on the ideas presented here would seem to require more sophisticated models of the target and array shape motions over time. For instance, targets could be limited to having known speeds and turning rates or hydrodynamic calculations of the array behaviour could be used to improve on the modelling of its shape.

## References


[1] T. Back, F. Hoffmeister, and H.-P. Schwefel. A survey of evolution strategies. In R. K. Belew and L. B. Booker, editors, *Proceedings of the 4th International Conference on Genetic Algorithms (ICGA IV)*, pages 2–9, San Diego, 1991. Morgan Kaufman Publishers, Inc.

[2] S. Baluja. *Population-Based Incremental Learning: A Method for Integrating Genetic Search Based Function Optimization and Competitive Learning.* Carnegie Mellon University, 1994.

[3] M.J. Box. A new method of constrained optimization and a comparison with other methods. *Comp. J.*, 8:42–52, 1965.

[4] L. Davis. Bit-climbing, representational bias, and test suite design. In R. K. Belew and L. B. Booker, editors, *Proceedings of the 4th International Conference on Genetic Algorithms (ICGA IV)*, pages 18–23, San Diego, 1991. Morgan Kaufman Publishers, Inc.

[5] NAg E04UCF. *NAg Mark 14 Reference Manual.* Numerical Algorithms Group Ltd., Oxford, 1990.

[6] D.J. Edwards and P.M. Terrell. The smoothed step track antenna controller. *Int. J. Satellite Comms.*, 1(1):133–139, 1981.

[7] D.D. Feldman and L.J. Griffiths. A projection approach for robust adaptive beamforming. *IEEE Trans. on Signal Processing*, 42(4):867–876, 1994.

[8] D.B. Fogel. Applying evolutionary programming to selected traveling salesman problems. *Cybernetics and Systems*, 24(1):27–36, 1993.

[9] W.R. Hahn. Optimum signal processing for passive sonar range and bearing estimation. *J. Acoust. Soc. Am.*, 58(1):201–207, 1975.

[10] S. Haykin, J.H. Justice, N.L. Ouisley, J.L. Yen, and A.C. Kak. *Array Signal Processing.* Prentice Hall, 1985.

[11] D.H. Johnson. The application of spectral estimation methods to bearing estimation problems. *Proc. I.E.E.*, 70(9):1018–1028, 1982.

[12] A.J. Keane. *The OPTIONS concept design system user manual.* Dynamics Modelling Ltd., 1993.

[13] A.J. Keane. Experiences with optimizers in structural design. In I.C. Parmee, editor, *Proceedings of the Conference on Adaptive Computing in Engineering Design and Control 94*, pages 14–27, Plymouth, U.K., 1994. University of Plymouth, P.E.D.C.

[14] A.J. Keane. Passive vibration control via unusual geometries: the application of genetic algorithm optimization to structural design. *J. Sound Vib.*, 185(3):441–453, 1995.

[15] S. Kirkpatrick, C.D. Gelatt, Jr., and M.P. Vecchi. Optimization by simulated annealing. *Science*, 220(4598):671–680, 1983.

[16] S.J. Marcos. Calibration of a distorted towed array using a propagation vector. *J. Acoust. Soc. Am.*, 93(4)(1):1987–1994, 1993.

[17] J.A. Nelder and R. Meade. A simplex method for function minimization. *Computer J.*, 7:308–313, 1965.

[18] B.P. Ng, M.H. Er, and C. Kot. Array gain/phase calibration techniques for adaptive beamforming and direction finding. *IEE Proc Radar, Sonar Navigation*, 141(1):25–29, 1994.

[19] L.A. Pflug, G.E. Loup, J.W. Loup, R.L. Field, and J.H. Leclere. Time delay estimation for deterministic transients using second and higher order correlations. *J. Acoust. Soc. Am.*, 94(3)(1):1385–1399, 1993.

[20] W.H. Press, B.P. Flannery, S.A. Teukolsky, and W.T. Vetterling. *Numerical Recipes: the Art of Scientific Computing*. Cambridge University Press, 1986.

[21] H.H. Rosenbrock. An automatic method for finding the greatest or least value of a function. *Comp. J.*, 3:175–184, 1960.

[22] H.-P. Schwefel. *Evolution and Optimum Seeking*. John Wiley and Sons, 1995.

[23] J.N. Siddall. *Optimal Engineering Design: Principles and Applications*. Marcel Dekker, Inc., 1982.

[24] C.J. Tsai and J.F. Yang. Autofocussing technique for adative coherent signal-subspace transformatio beamformers. *IEE Proc Radar, Sonar Navigation*, 141(1):30–36, 1994.

[25] D. Yuret and M. de la Maza. Dynamic hill climbing: Overcoming the limitations of optimization techniques. In *Proceedings of the 2nd Turkish Symposium on AI and ANN*, pages 254–260, 1993.